Simple and direct measurements of pretilt angles in hybrid-aligned nematic liquid-crystal cells

Sheng-Ya Wang,[1,*] Huang-Ming Wu,[2] and Kei-Hsiung Yang[3]

[1]Institute of Photonic Systems, National Chiao Tung University, No. 301, Gaofa 3rd Road, Guiren District, Tainan City 711, Taiwan

[2]Institute of Lighting and Energy Photonics, National Chiao Tung University, No. 301, Gaofa 3rd Road, Guiren District, Tainan City 711, Taiwan

[3]Institute of Imaging and Biomedical Photonics, National Chiao Tung University, No. 301, Gaofa 3rd Road, Guiren District, Tainan City 711, Taiwan

*Corresponding author: shengyawang@gmail.com

Received 8 May 2013; revised 18 June 2013; accepted 20 June 2013;
posted 21 June 2013 (Doc. ID 190122); published 15 July 2013

We have developed a general approach to perform direct measurements of the pretilt angles from 0° to 75° in hybrid-aligned nematic (HAN) liquid-crystal cells whose cell gaps can also be accurately determined with the help of known pretilt angles. In this paper, we have used a Zeeman laser system to measure the angular-dependence phase retardation of the HAN cells and MATLAB mathematical software to carry out theoretical calculations and fit the measured data to derive the pretilt angles. In general, pretilt angles adjacent to opposite substrates of a HAN cell are different. Our measured pretilt angles of the HAN cell were in good agreement with the measured pretilt angles of two accompanying homogenous cells whose alignment methods were the same as applied to opposite substrates of the HAN cell, respectively. The advantage of direct measurement is easily applicable to measure the pretilt angles of aged HAN cells. © 2013 Optical Society of America

OCIS codes: (160.3710) Liquid crystals; (230.3720) Liquid-crystal devices; (120.5050) Phase measurement.

http://dx.doi.org/10.1364/AO.52.005106

1. Introduction

The hybrid-aligned nematic (HAN) liquid-crystal (LC) mode has attracted much attention in recent years due to its thresholdless driving voltage and slow variation of birefringence with voltage [1], which are important characteristics for transflective displays and LC lenses. The pretilt angles are important parameters to strongly affect the electro-optic effects of HAN cells. In general, the pretilt angles of a HAN cell are different at opposite substrates of the cell. In this case, as a common practice, the pretilt angles of a HAN cell were inferred from the measured pretilt angles of two accompanying homogeneous cells whose alignment methods were the same as applied to opposite substrates of the HAN cell, respectively. The pretilt angles of accompanying homogenous cells were usually measured by the well-recognized crystal rotation method [2]. However, the pretilt angles of aged HAN cells after consumer use in the field could not be inferred from the pretilt angles of aged accompanying homogenous cells in the laboratory due to different aging processes. In this paper, we provide a simple method to directly measure the pretilt angles of HAN LC cells extendable to aged ones.

Regarding the published methods to measure the pretilt angles of HAN cells, Hung *et al.* [3] and Ishinabe *et al.* [4] have proposed curve fitting

1559-128X/13/215106-06$15.00/0

methods to determinate cell parameters of HAN cells. However, both methods used pretilt angles and cell gaps as fitting parameters in their fitting equations. In general, the pretilt angles and cell gap are entangled in the phase retardation Γ as shown in Eq. (1). Therefore, the errors of derived pretilt angles and cell gap were interdependent unless the empty cell gap was measured independently before LC injection into the HAN cell and remained unchanged thereafter. In addition, Ishinabe *et al.* [4] utilized complicated calculations based on the extended Jones matrix to derive cell parameters of HAN cells. It was difficult to program the fitting functions to obtain accurate results due to complicated formulas. On the other hand, Fuh *et al.* [5] also derived the pretilt angles of HAN cells by comparing the measured voltage-versus-transmission curve (V–T curve) with the calculated results using 1D-DIMOS software. In our opinion, this method was inaccurate for the determination of pretilt angles of HAN cells if the pretilt angles adjacent to opposite cell substrates were different.

In this paper, we report simple and direct measurements of the pretilt angles as well as the cell gaps of HAN cells. Compared to the published curve fitting method [3,4], our method is simpler and suitable for a wider range of pretilt angles from 0° to 75° extendable to 0° to 90°. For the measurements of phase retardation as a function of incident angle, we have used an experimental scheme of out-of-plane cell rotation. We have developed a new model of data analysis by comparing the calculated and measured phase retardations of the HAN cells. In addition, the equations were functions of pretilt angles rather than a simultaneous function of pretilt angles and cell gap. Using our method of measurement, we have obtained pretilt angles of freshly made HAN cells in good agreement with those measured on the accompanying freshly made homogenous cells by the well-accepted crystal rotation method [2]. The alignment films of the accompanying homogenous cells were made using the same materials and process steps as those to fabricate the HAN cells. We believe that our method of direct measurement can be easily extended to measure the pretilt angles of aged HAN cells.

2. Theory

In order to determine the pretilt angles of HAN cells, we have to calculate the phase retardation of the HAN cell in different incident angles. Figure 1 shows the director profile of LC molecules of the HAN cell, and θ_1 and θ_2 are the surface pretilt angles on the bottom and top substrates, respectively. We then divide the HAN cell into n layers ($n = 1000$), and each layer can be approximated by a homogenous LC cell with a different tilt angle for LC directors within that layer. Based on the Oseen–Frank elastic continuum theory for nematic LCs, the variation of pretilt angles within the HAN cell is a linear function of z under the condition that elastic constant K_{11} is

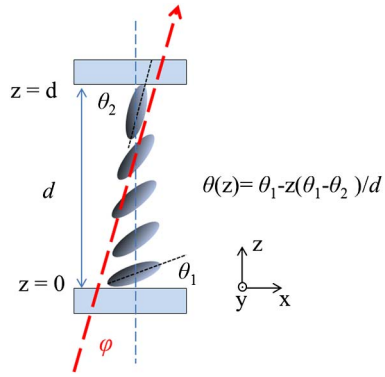

Fig. 1. Director profile of LC molecules in a HAN cell.

equal to K_{33}. In the experiment, E7 was used as LC material in HAN cells. Although the elastic constant K_{11} is not equal to K_{33} in E7, we simplify the calculation for the orientations of LC directors within a HAN cell by assuming that the orientations can be approximated by a linear function of z when the cell gap is sufficiently large. Our above assumption might have been oversimplified if the subsequently obtained results of the pretilt angles of HAN cells had not been in good agreement with the measured pretilt angles of two accompanying homogenous cells whose methods of alignment were the same as applied to opposite substrates of the HAN cell, respectively. Therefore, we let $\theta(z)$ denote the LC-director tilt angle for the LC layer located at position z and $\theta(z) = \theta_1 - z(\theta_1 - \theta_2)/d$, where d is the cell gap of the HAN cell. Scheffer and Nehring [2] have calculated the phase retardation as function of the incident angle for the homogenously aligned LC cell, and the result is shown in Eq. (1), where n_o and n_e are the ordinary and extraordinary indices of refraction of the LC medium, respectively, θ is tilt angle of the LC director, and φ is the incident angle of the light. The total phase retardation, Γ_{total}, of the HAN cell can be expressed as a function of cell gap, d, pretilt angles, θ_1 and θ_2, and incident angle φ as shown below:

$$\Gamma = \frac{2\pi \Delta d}{\lambda}\left[\frac{(n_o^2 - n_e^2)\sin\theta\cos\theta}{n^2} \times \sin\varphi + \frac{n_o n_e\sqrt{n^2 - \sin^2\varphi}}{n^2} - \sqrt{n_o^2 - \sin^2\varphi}\right], \quad (1)$$

where

$$n^2 = n_o^2\cos^2\theta + n_e^2\sin^2\theta,$$

$$\Gamma_{\text{total}}(d,\theta_1,\theta_2,\varphi) = \int_{\theta_1}^{\theta_2}\frac{2\pi d}{\lambda(\theta_2-\theta_1)} \times \left[\frac{(n_o^2 - n_e^2)\sin\theta\cos\theta}{n^2}\sin\varphi + \frac{n_o n_e\sqrt{n^2 - \sin^2\varphi}}{n^2} - \sqrt{n_o^2 - \sin^2\varphi}\right]d\theta. \quad (2)$$

For the sake of solving the pretilt angles, θ_1 and θ_2, we define χ_1 and χ_2 as the ratio of total phase retardation at incident angle $\pm\varphi_1$, $\pm\varphi_2$, respectively, resulting in χ_1 and χ_2 being functions of pretilt angles rather than a simultaneous function of pretilt angles and cell gap. We then measure the phase retardations at different incident angles $\pm\varphi_1$, $\pm\varphi_2$ for the HAN cells using the heterodyne interference method [6], and solve Eqs. (3) and (4) for the pretilt angles of the HAN cell using MATLAB mathematical software:

$$\chi_1(\theta_1,\theta_2,\pm\varphi_1)=\frac{\Gamma_{\text{total}}(\theta_1,\theta_2,-\varphi_1)}{\Gamma_{\text{total}}(\theta_1,\theta_2,\varphi_1)}, \tag{3}$$

$$\chi_2(\theta_1,\theta_2,\pm\varphi_2)=\frac{\Gamma_{\text{total}}(\theta_1,\theta_2,-\varphi_2)}{\Gamma_{\text{total}}(\theta_1,\theta_2,\varphi_2)}. \tag{4}$$

Using Eqs. (3) and (4), the pretilt angles of any HAN cells can be derived. However, for pretilt angles in some region, such as $\theta_1 < 25°$ and $\theta_2 > 80°$, χ_1 and χ_2 are insensitive to changes in the pretilt angles of HAN cells, resulting in large errors of measurement as shown in Fig. 2. In these situations, we have to modify Eqs. (3) and (4) to increase their sensitivities with respect to the change in the pretilt angles of HAN cells, as will be explained in the following section.

3. Simulations

We use MATLAB mathematical software to calculate χ_1 and χ_2. LC-cell parameters used in the simulation are shown in Table 1. We then use Eq. (3) to plot χ_1 versus θ_1 with θ_2 treating $\varphi_1 = 40°$ as a parameter. The results are shown in Fig. 2, indicating that χ_1 is insensitive to pretilt angles in a region in which θ_1 is below 25° and θ_2 is larger than 80°. In this case, the measured pretilt angles will have substantial errors when Eqs. (3) and (4) are used in such a region in which θ_1 is below 25° and θ_2 is larger than 80°. For the purpose of modifying the equations, we calculate

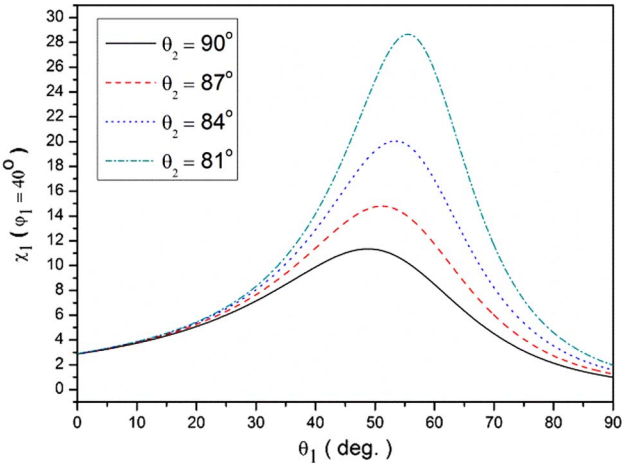

Fig. 2. χ_1 versus θ_1 with θ_2 as a parameter with $\varphi_1 = 40°$.

Table 1. LC Parameters Used in the Calculations

Refractive Index		Cell gap (μm)	Wavelength λ (nm)
n_e	1.75	9	633
n_o	1.523		

the phase retardation versus the incident angle of HAN cells by fixing the pretilt angle on bottom glass substrates at 5° and changing θ_2 from 81° to 90°. The results are shown by the inserted figure in Fig. 3. It indicates that the phase retardation of a HAN cell converged at large positive incident angles. Hence, there exist improved equations, Eqs. (5) and (6), to make modified χ sensitive to the deviation of pretilt angle in such a region. Figure 3 also shows χ_3 versus θ_1 with θ_2 using $\varphi_1 = 40°$ and $\varphi_2 = 50°$ as parameters, indicating that χ_3 is more sensitive than χ_1 in the region in which θ_1 is below 25° and θ_2 is larger than 80°. In the case in which pretilt angles of HAN cells have θ_1 lower than 25° and θ_2 higher than 80°, Eqs. (5) and (6) are utilized to reduce the measurement error. Consequently, by choosing any two equations as a pair from Eqs. (3)–(6), we believe that all of the pretilt angles of HAN cells can be derived with good accuracy. After accurate pretilt angles of a HAN cell are determined, we can derive the cell gap of the HAN cell with good accuracy directly from Eq. (2):

$$\chi_3(\theta_1,\theta_2,\pm\varphi_1,\pm\varphi_2)=\frac{\Gamma_{\text{total}}(\theta_1,\theta_2,-\varphi_1)}{\Gamma_{\text{total}}(\theta_1,\theta_2,\varphi_1)-\Gamma_{\text{total}}(\theta_1,\theta_2,\varphi_2)}, \tag{5}$$

$$\chi_4(\theta_1,\theta_2,\pm\varphi_1,\pm\varphi_2)=\frac{\Gamma_{\text{total}}(\theta_1,\theta_2,-\varphi_2)}{\Gamma_{\text{total}}(\theta_1,\theta_2,\varphi_1)-\Gamma_{\text{total}}(\theta_1,\theta_2,\varphi_2)}. \tag{6}$$

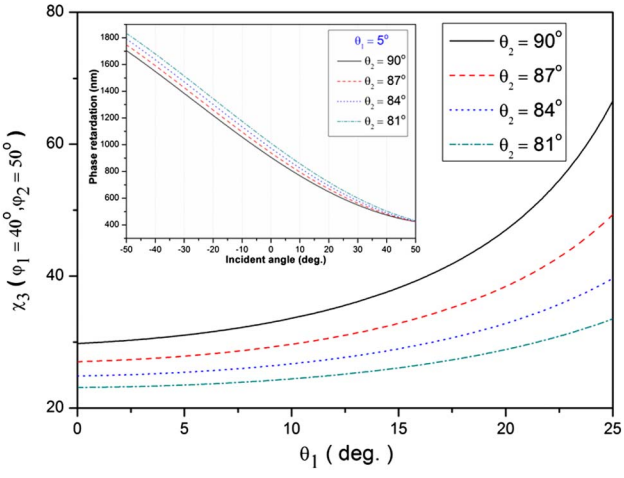

Fig. 3. χ_3 versus θ_1 with θ_2 as a parameter with $\varphi_1 = 40°$ and $\varphi_2 = 50°$. The inserted figure denotes phase retardation versus incident angle with $\theta_1 = 5°$ and changing θ_2 from 81° to 90°.

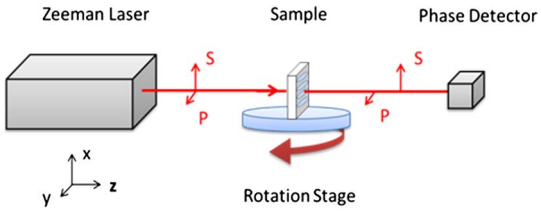

Fig. 4. Experimental scheme to measure phase retardations of HAN cells.

4. Experiments

Our samples were prepared by a standard cell fabrication process. HAN cells were composed of a nematic LC (E7) sandwiched between two parallel rubbed alignment films with high and low pretilt angles on ITO-coated glass substrates, respectively. In some of our samples, we doped the homogeneous-alignment film (HAF) with the nanoparticle polyhedral oligomeric silsesquioxane (POSS) to change the pretilt angles of HAN cells. Our goal was to measure the pretilt angles of HAN cells so that we used HAF (AL-58, Daily polymer Cop.) doped with 0.07 wt. % of the nanoparticle POSS as tunable alignment films (TAFs) [7]. By changing the rubbing depth, we could control the pretilt angles of TAF from 3° to 75° in each HAN cell as shown in Tables 3, 5, and 6. The HAN samples were composed of TAF on one side and HAF or vertical-alignment film (VAF) at the opposite side. HAF and VAF were fabricated by coating homogenously aligned polyimide and vertically aligned polyimide on glass substrate and using a rubbing machine to make the polymer chains aligned. In an attempt to compare the pretilt angles of homogenous cells with those of HAN cells, a HAN cell and two accompanying homogenous cells were fabricated by the same LC-cell process with the same batch of ball spacers (average diameter = 8 μm) and the same nematic LC mixture. Two accompanying homogenous cells were assembled by two antiparallel aligned HAFs and VAFs, respectively.

For the measurements of pretilt angles, we applied a heterodyne interference method using a Zeeman laser system [6] to measure the phase retardations versus incident angles as shown in Fig. 4. We did not consider the multiple-beam interference inside the cell by using such a method for measurements of phase retardations of LC cells. The sample was placed on a rotation stage with rubbing direction parallel to the y axis. We measured the phase retardations of the HAN cells at $\varphi = \pm 50°$, $\pm 40°$, and $\pm 30°$. For comparison, we also followed Scheffer's experimental scheme [2] of crystal rotation to measure phase retardations versus incident angles for homogenous cells to determine their pretilt angles.

Table 2. Phase Retardations of HAN Cells at Different Incident Angles

Incident Angle	Phase Retardation $A_{TAF\text{-}VAF}$	Phase Retardation $B_{TAF\text{-}VAF}$	Phase Retardation $C_{TAF\text{-}VAF}$	Phase Retardation $D_{TAF\text{-}VAF}$	Phase Retardation $E_{TAF\text{-}VAF}$	Phase Retardation $F_{TAF\text{-}VAF}$
−50°	14.61	15.32	22.24	12.42	11.96	6.70
−40°	13.64	13.79	19.33	10.16	9.41	5.08
−30°	11.87	12.58	16.43	8.91	7.62	3.56
30°	4.85	4.64	3.72	1.79	0.92	0.53
40°	4.20	3.98	2.91	1.33	0.81	1.18
50°	3.79	3.56	2.67	1.32	0.98	2.13

Table 3. Measured Pretilt Angles of HAN Cells and Vertically Aligned Cells

	Sample $A_{TAF\text{-}VAF}$	Sample $B_{TAF\text{-}VAF}$	Sample $C_{TAF\text{-}VAF}$	Sample $D_{TAF\text{-}VAF}$	Sample $E_{TAF\text{-}VAF}$	Sample $F_{TAF\text{-}VAF}$
Pretilt angle of TAF	$3.1 \pm 0.4°$	$10.9 \pm 0.6°$	$25.6 \pm 0.5°$	$33.5 \pm 0.3°$	$43.8 \pm 0.5°$	$70.9 \pm 0.6°$
Pretilt angle of VAF	$89.3 \pm 0.3°$	$89.3 \pm 0.3°$	$89.3 \pm 0.3°$	$89.3 \pm 0.3°$	$89.3 \pm 0.3°$	$89.3 \pm 0.3°$
Pretilt angles of HAN cell	$3.5 \pm 0.3°$/ $89.6 \pm 0.2°$	$10.5 \pm 0.1°$/ $89.4 \pm 0.1°$	$27.7 \pm 0.1°$/ $89.2 \pm 0.3°$	$32.7 \pm 0.3°$/ $89.5 \pm 0.3°$	$42.2 \pm 0.8°$/ $88.6 \pm 0.4°$	$70.5 \pm 0.8°$/ $89 \pm 0.4°$

Table 4. Phase Retardations of HAN cells at Different Incident Angles

Incident Angle	Phase Retardation $A_{TAF\text{-}HAF}$	Phase Retardation $B_{TAF\text{-}HAF}$	Phase Retardation $C_{TAF\text{-}HAF}$	Phase Retardation $D_{TAF\text{-}HAF}$	Phase Retardation $E_{TAF\text{-}HAF}$
−50°	19.19	20.11	27.10	19.08	16.54
−40°	18.93	19.79	26.32	18.01	15.39
−30°	18.51	19.36	25.17	16.85	14.11
30°	12.34	12.73	13.84	8.27	6.19
40°	10.93	11.31	11.81	7.01	5.20
50°	9.62	9.83	10.07	5.91	4.43

Table 5. Measured Pretilt Angles of HAN Cells and Homogenously Aligned Cells

	Sample $A_{TAF\text{-}HAF}$	Sample $B_{TAF\text{-}HAF}$	Sample $C_{TAF\text{-}HAF}$	Sample $D_{TAF\text{-}HAF}$	Sample $E_{TAF\text{-}HAF}$
Pretilt angle of TAF	$28.7 \pm 0.4°$	$33.0 \pm 0.6°$	$45.1 \pm 0.3°$	$58.3 \pm 0.3°$	$70.7 \pm 0.5°$
Pretilt angle of HAF	$1.7 \pm 0.2°$	$1.7 \pm 0.2°$	$1.7 \pm 0.2°$	$1.7 \pm 0.2°$	$1.7 \pm 0.2°$
Pretilt angles of HAN cell	$1.9 \pm 0.3°$/ $29.6 \pm 0.6°$	$2.0 \pm 0.5°$/ $30.9 \pm 0.4°$	$2.1 \pm 0.3°$/ $46 \pm 0.2°$	$1.9 \pm 0.3°$/ $57.4 \pm 0.5°$	$1.3 \pm 0.55°$/ $71.2 \pm 0.3°$

Table 6. Phase Retardations and Calculated Pretilt Angles for TAF-Aligned HAN Cell

Incident Angle	Phase Retardation A_{TAF}		Sample $A_{TAF\text{-}HAF}$
−50°	14.09	Pretilt angle of TAF_{top}	$28.7 \pm 0.3°$
−40°	12.47		
−30°	10.76	Pretilt angle of TAF_{bottom}	$70.0 \pm 0.6°$
30°	2.44		
40°	1.73	Pretilt angles of HAN cell	$28.8 \pm 0.8°/70.7 \pm 0.4°$
50°	1.26		

Table 7. Measured Cell Gaps of HAN Cells

	Sample $A_{TAF\text{-}VAF}$	Sample $B_{TAF\text{-}VAF}$	Sample $C_{TAF\text{-}VAF}$	Sample $D_{TAF\text{-}VAF}$	Sample $E_{TAF\text{-}VAF}$	Sample $F_{TAF\text{-}VAF}$
Cell gap (μm)	8.69	8.47	8.86	8.26	8.75	8.57
	Sample $A_{TAF\text{-}HAF}$	Sample $B_{TAF\text{-}HAF}$	Sample $C_{TAF\text{-}HAF}$	Sample $D_{TAF\text{-}HAF}$	Sample $E_{TAF\text{-}HAF}$	
Cell gap (μm)	8.03	8.46	8.57	8.65	8.85	

5. Results and Discussion

First, we measured the HAN cells composed of TAF and VAF. A set of measured phase retardations for all samples is shown in Table 2. By choosing any two equations among Eqs. (3)–(6), we could solve the pretilt angles by selecting $\varphi = \pm 50°$, $\pm 40°$, and $\pm 30°$, respectively, shown in Table 3. The pretilt angles of corresponding accompanying homogenous cells are also shown in Table 3.

Second, we measured the HAN cell composed of TAF on one side of the cell and HAF on the other side. We also listed the measured phase retardations and calculated the pretilt angle for each cell using the proposed method shown in Tables 4 and 5, respectively.

Finally, we measured the HAN cell aligned by two TAFs with arbitrary pretilt angles on both sides of the HAN cell. The measured phase retardation and derived pretilt angles are shown in Table 6.

By comparing the measured pretilt angles of TAF-, VAF-, and HAF-aligned cells from Tables 3, 5, and 6, we conclude that the measured pretilt angles of HAN cells are in good agreement with the measured pretilt angles of corresponding accompanying homogenous cells. It is a valid proof on the relevancy of our method of measurements. The results show that our method is simple and accurate to perform direct measurements of the pretilt angles in HAN cells.

From the measured results on the pretilt angles of HAN cells and by using Eq. (2), the cell gap of each HAN cell can be obtained. The measured results on cell gaps are shown in Table 7. Although we used ball spacers with an average ball-spacer size of 8 μm to create cell gaps, the measured cell gaps showed small deviations from the average size of ball spacers. The deviations might be caused by using different pressures to assemble the cells with different ball-spacer densities within the cells.

6. Conclusion

Based on our experimental scheme and analytical equations, we report a simple and accurate method to perform direct measurements of the pretilt angles in HAN LC cells. On freshly made samples, our results show that the measured pretilt angles of HAN cells were in good agreement with the measured pretilt angles of corresponding accompanying homogenous cells. Our method of direct measurement has potential applications in optimizing the design of the HAN mode for LC lenses and LCDs for better performance, and can be easily extended to monitor the changing pretilt angles of commercially aged thin-film-transistor-driven HAN LC panels or LC lenses for better reliability. Our method can also be used to detect the pretilt angles of HAN cells [5] aligned by photoexposed TAF films.

References

1. S. Matsumoto, M. Kawamoto, and K. Mizunoya, "Field-induced deformation of hybrid-aligned nematic liquid crystals: New multicolor liquid crystal display," J. Appl. Phys. **47**, 3842–3845 (1976).
2. T. J. Scheffer and J. Nehring, "Accurate determination of liquid crystal tilt bias angles," J. Appl. Phys. **48**, 1783–1792 (1977).
3. L. T. Hung, S. Oka, M. Kimura, and T. Akahane, "Determination of polar anchoring strength at vertical alignment nematic

liquid crystal-wall interface using thin hybrid alignment nematic cell," Jpn. J. Appl. Phys. **43**, L649–L651 (2004).
4. T. Ishinabe, Y. Ohno, T. Miyashita, and T. Uchida, "High-precision measurement of polar anchoring strength and elastic constant ratio using hybrid alignment nematic cell," Jpn. J. Appl. Phys. **47**, 8892–8897 (2008).
5. A. Y. G. Fuh, C. K. Liu, K. T. Cheng, C. L. Ting, and C. C. Chen, "Variable liquid crystal pretilt angles generated by photoalignment in homeotropically aligned azo dye-doped liquid crystals," Appl. Phys. Lett. **95**, 161104 (2009).
6. S. J. Hwang, "Precise optical retardation measurement of nematic liquid crystal display using the phase-sensitive technique," J. Display Technol. **1**, 77–81 (2005).
7. S. J. Hwang, S. C. Jeng, and I. M. Hsieh, "Nanoparticle-doped polyimide for controlling the pretilt angle of liquid crystals devices," Opt. Express **18**, 16507–16512 (2010).